

Neutron detector efficiency defined by the relative neutron yield in the deuteron photodisintegration process.

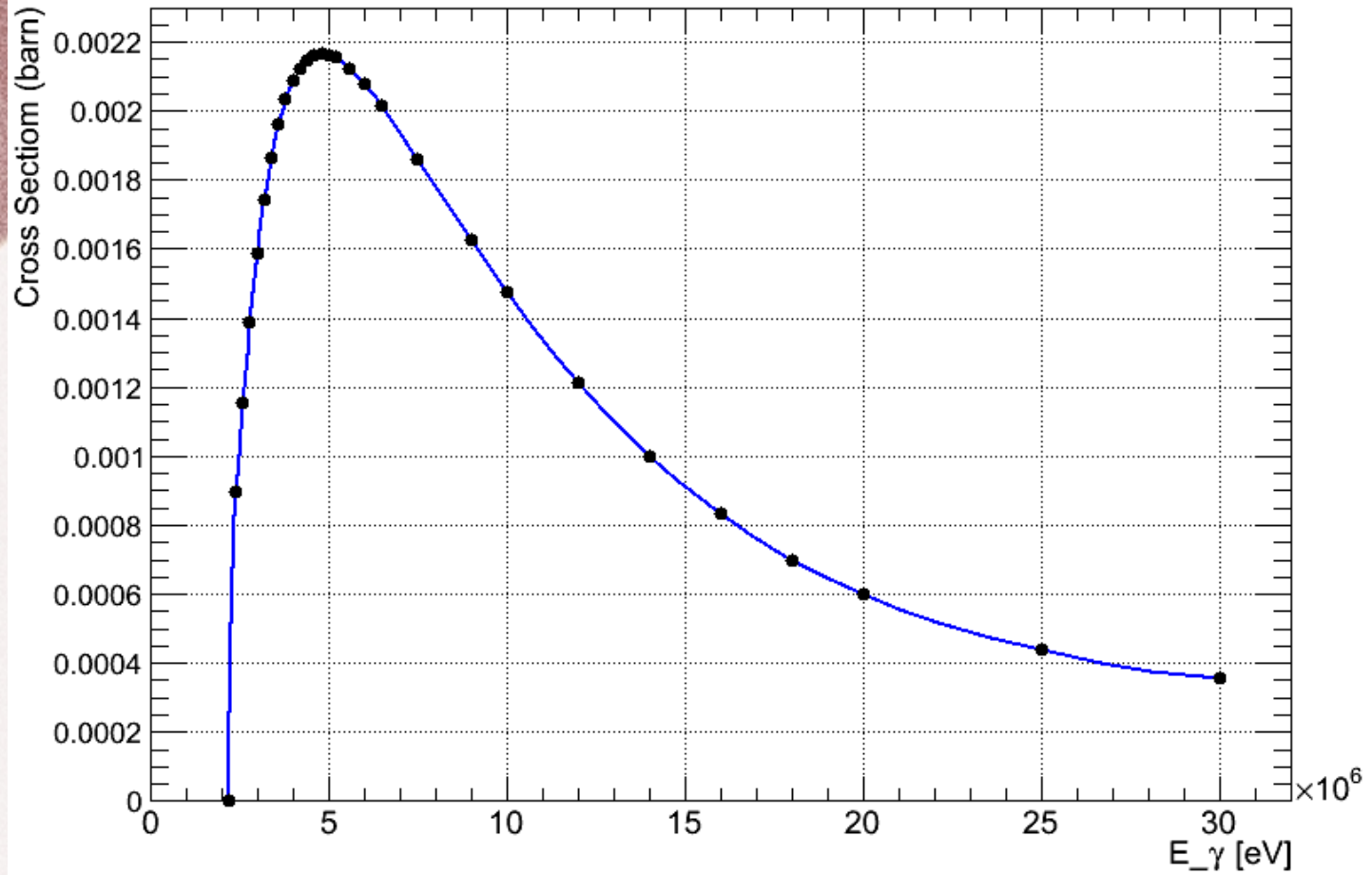


Fig. 1. Total cross section of H-2(γ ,absorption).
ENDF /B-VII.1.

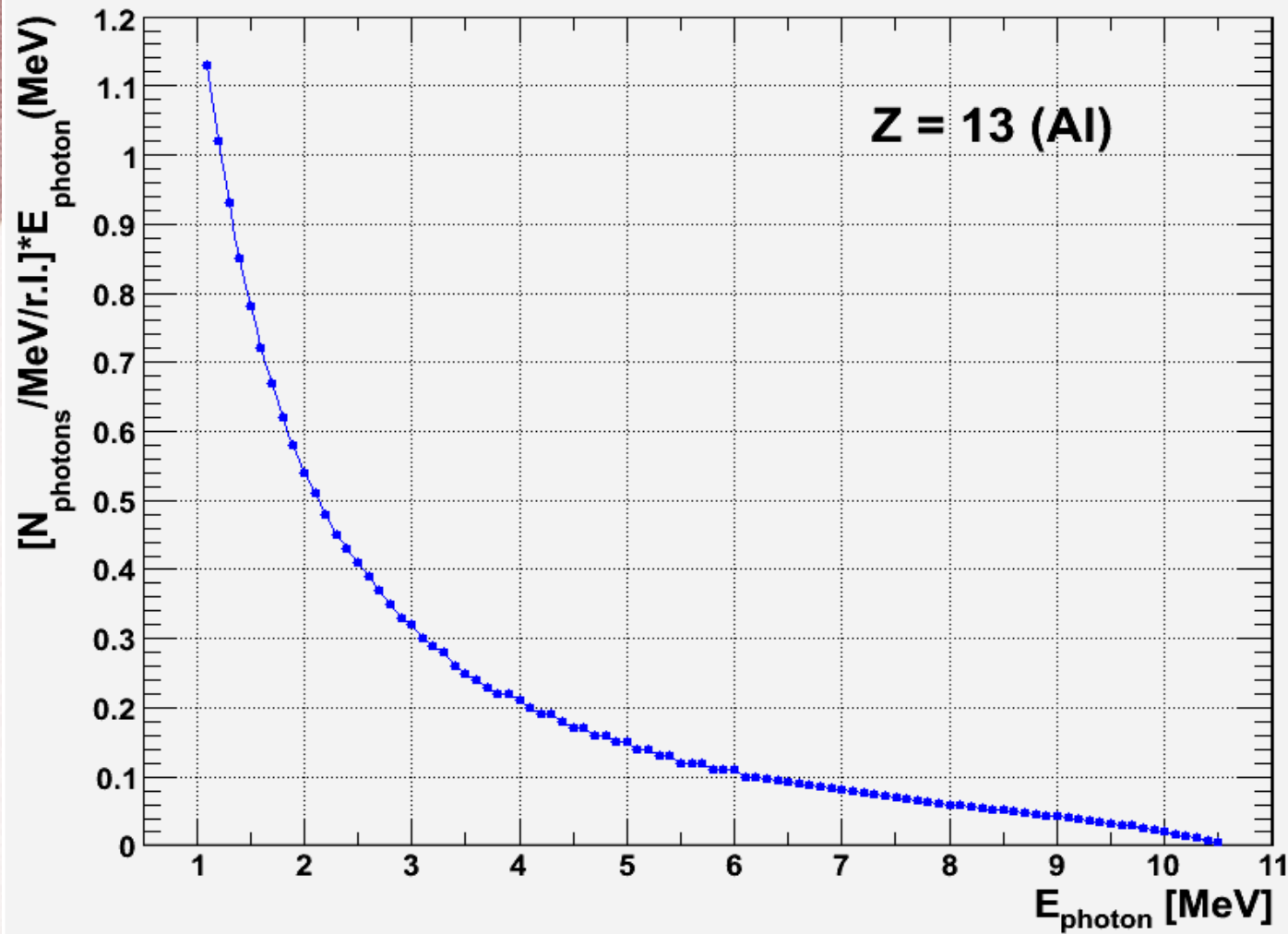


Fig. 2. Bremsstrahlung spectrum created by electrons with energy 10.5 MeV in aluminium converter [by Dr. Dale]

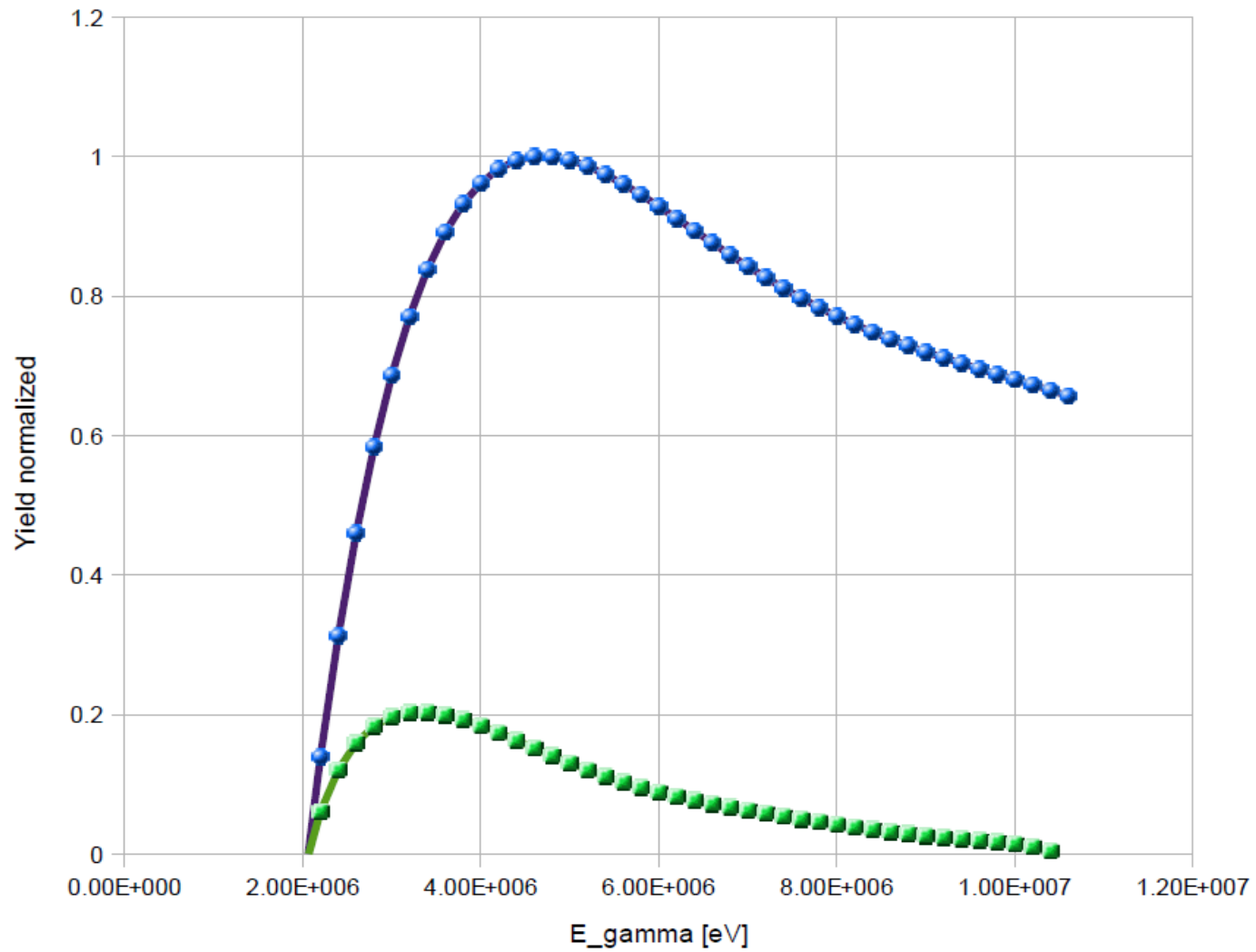


Fig. 3. Total crosssection of $\text{H-2}(\gamma,\text{absorption})$ reaction weighted by the bremsstrahlung spectrum (green curve) .

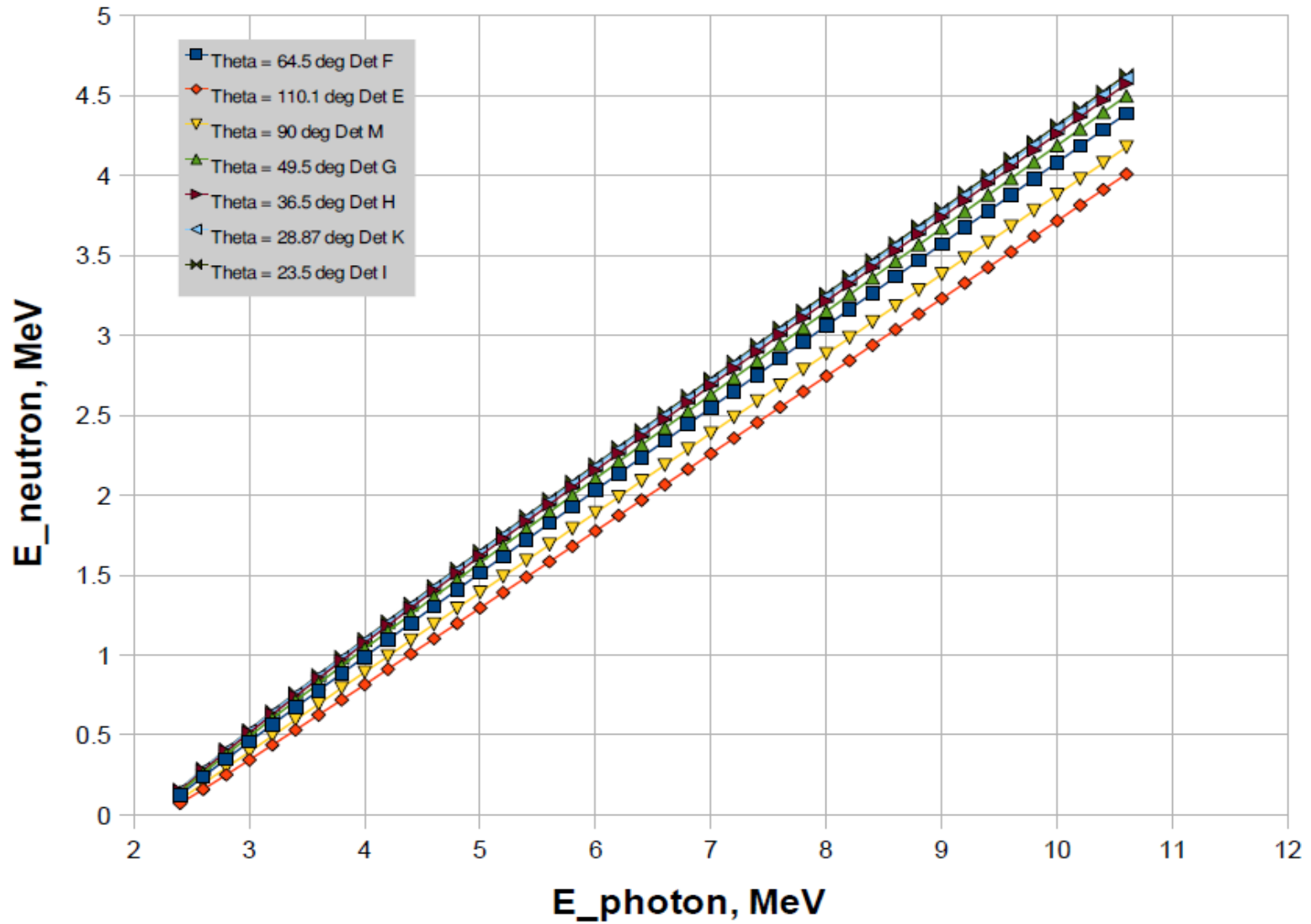


Fig. 4. Neutron energy vs. photon energy in the lab frame calculated using kinematics of the photodisintegration reaction.

$$\frac{d\sigma}{d\Omega} = A_y + B_y \sin^2(\theta) + C_y \sin^2(\theta) \cos(\theta) + D_y \sin^2(\theta) \cos^2(\theta)$$

E1, E2, M1 multipolarities are included [*]

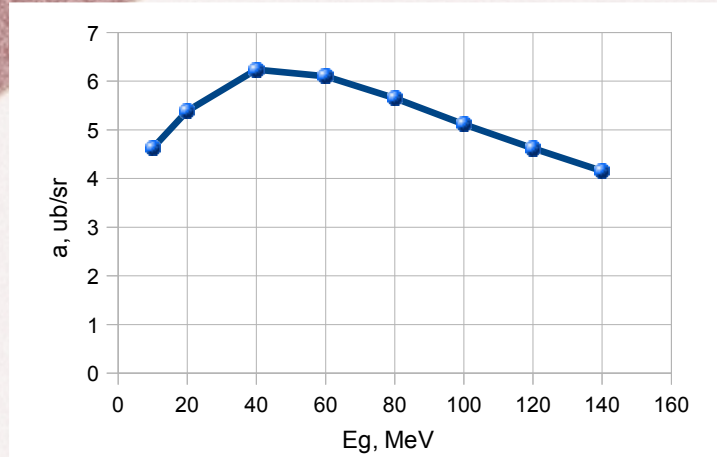


Fig. 5a. Coefficient A_y [**] F. Partovi, Ann. Phys. 27, 79 (1964)

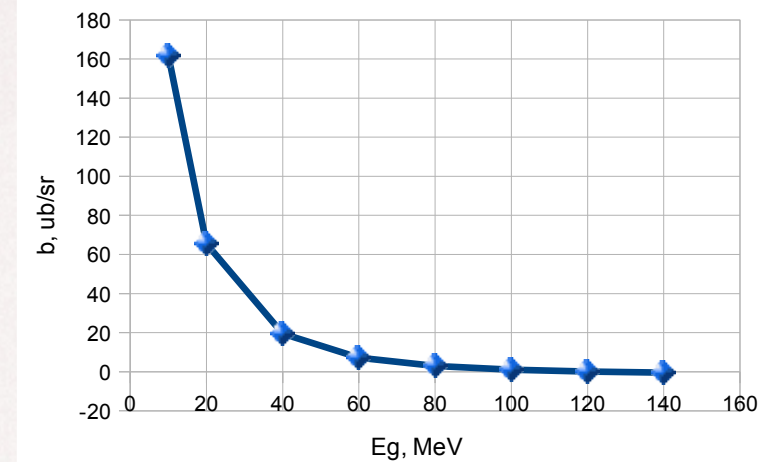


Fig. 5b. Coefficient B_y [**]

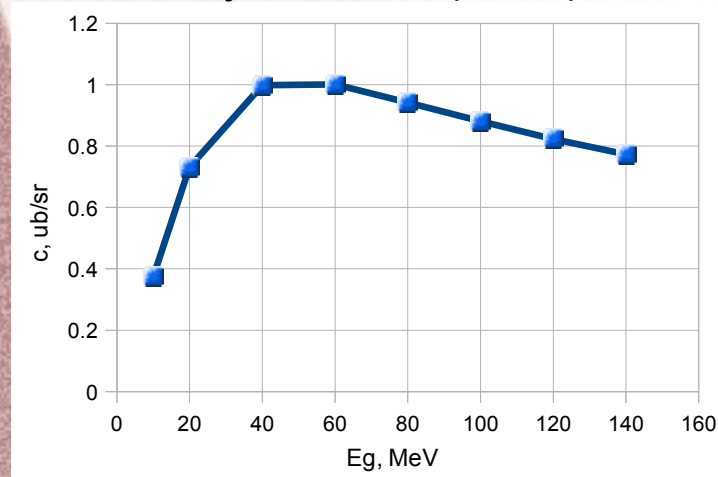


Fig. 5c. Coefficient C_y [**]

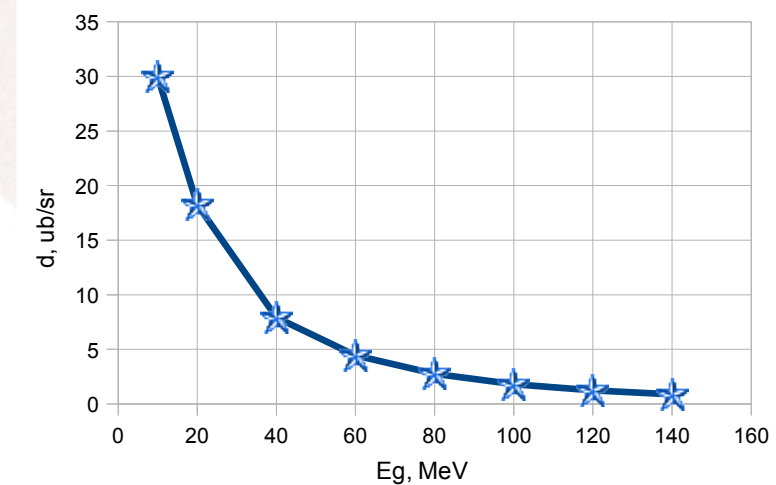


Fig. 5d. Coefficient D_y [**]

Partovi's coefficients after fitting

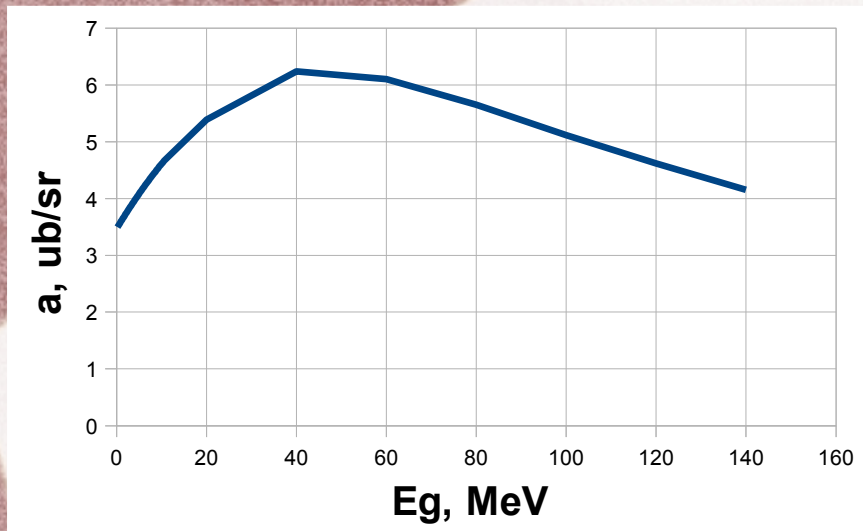


Fig. 6a. Coefficient A_{γ} .

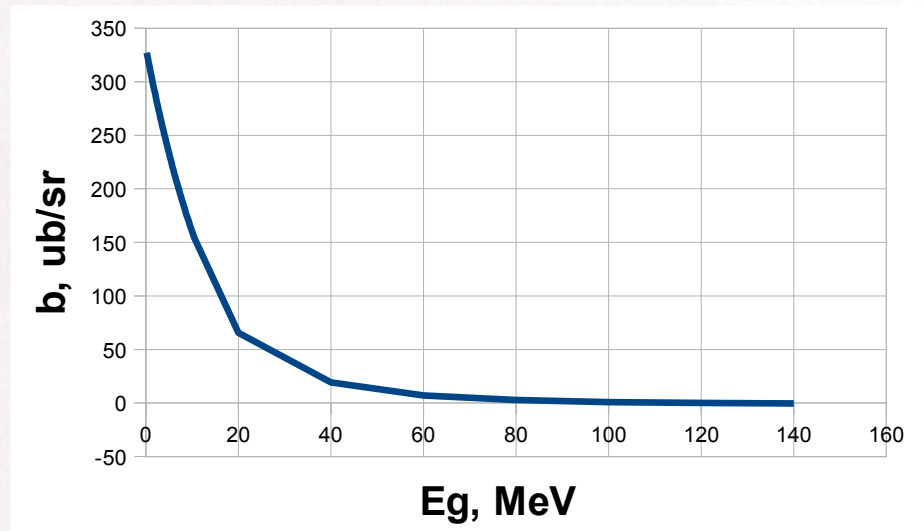


Fig. 6b. Coefficient B_{γ} .

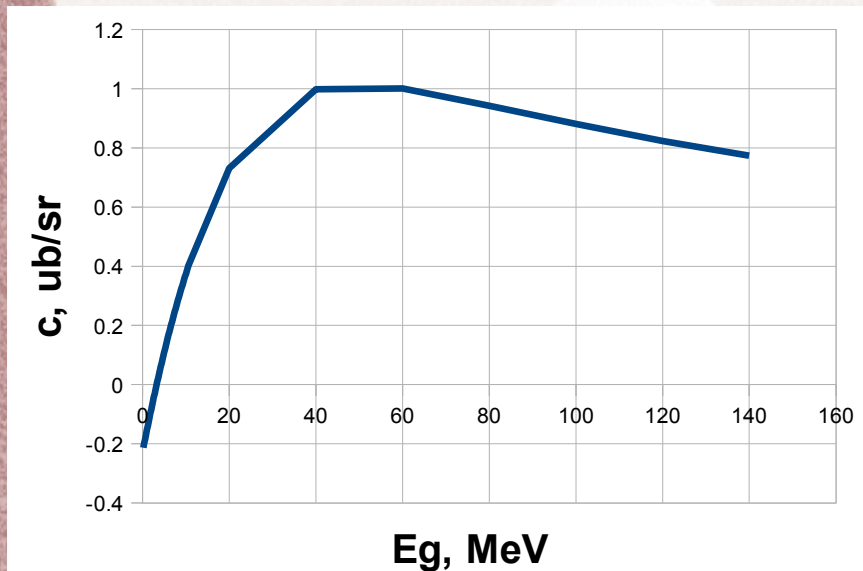


Fig. 6c. Coefficient C_{γ} .

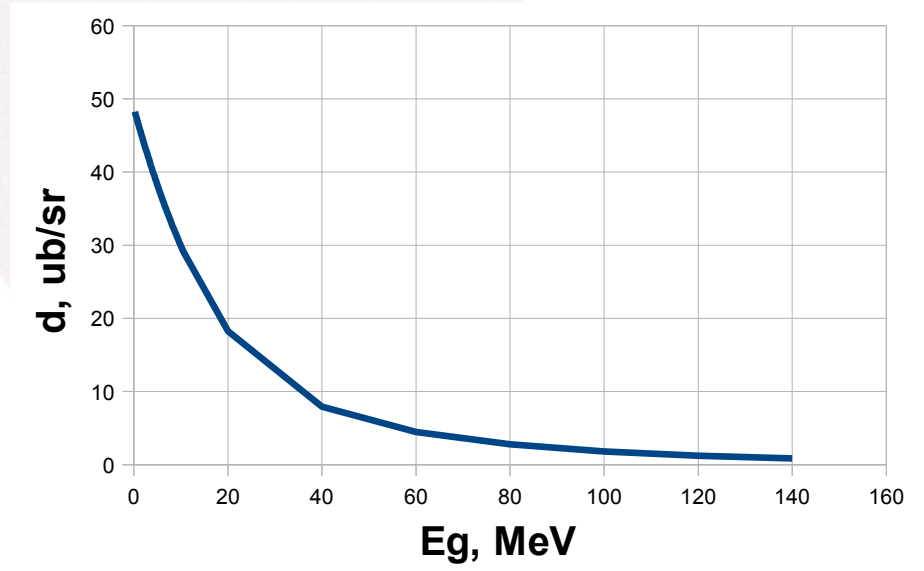


Fig. 6d. Coefficient D_{γ} .

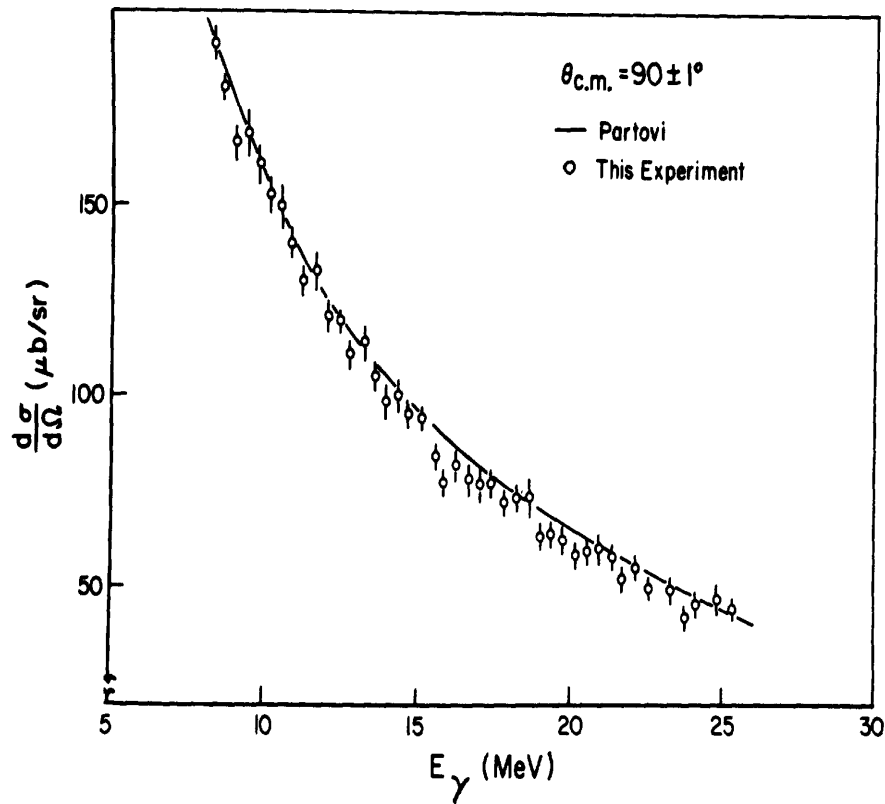


FIG. 7. Differential cross section at a c.m. angle of $90 \pm 1^\circ$. The errors shown are statistical only.

[*] D. M. Skopik, Y. M. Shin, M. C. Phenneger, J. J. Murphy, *Photodisintegration of deuteron determined from the electrodisintegration process*, Phys. Rev. C, Vol. 9, 2, February 1974.

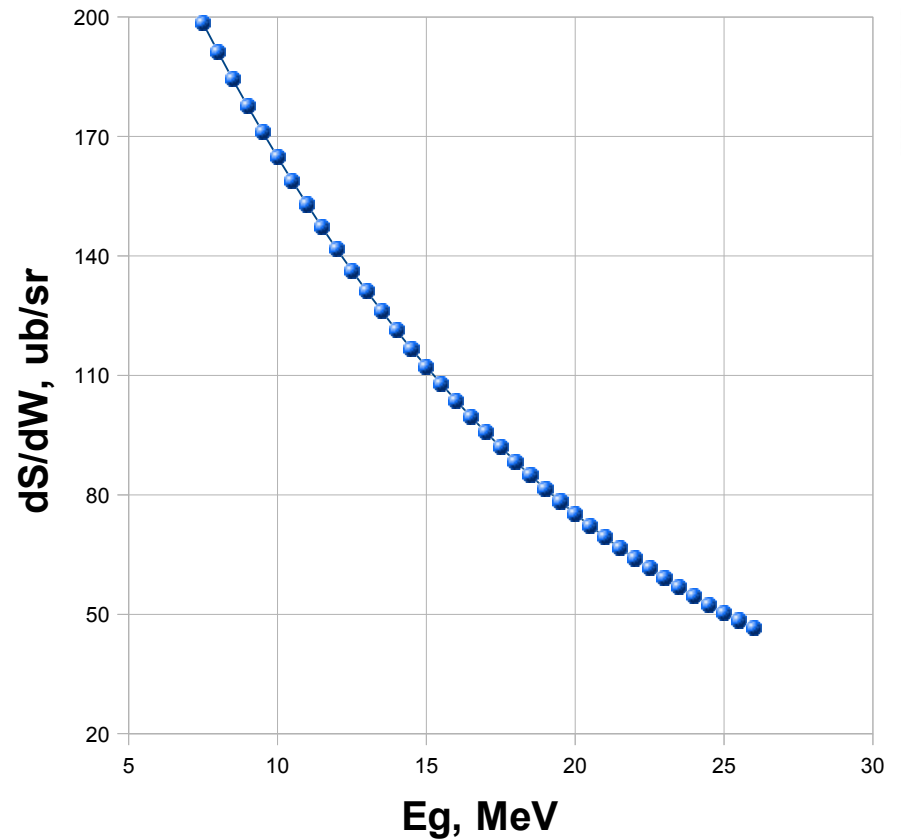


Fig. 8. Reproduction of the data plotted in Fig. 7 using fitted Partovi's coefficients.

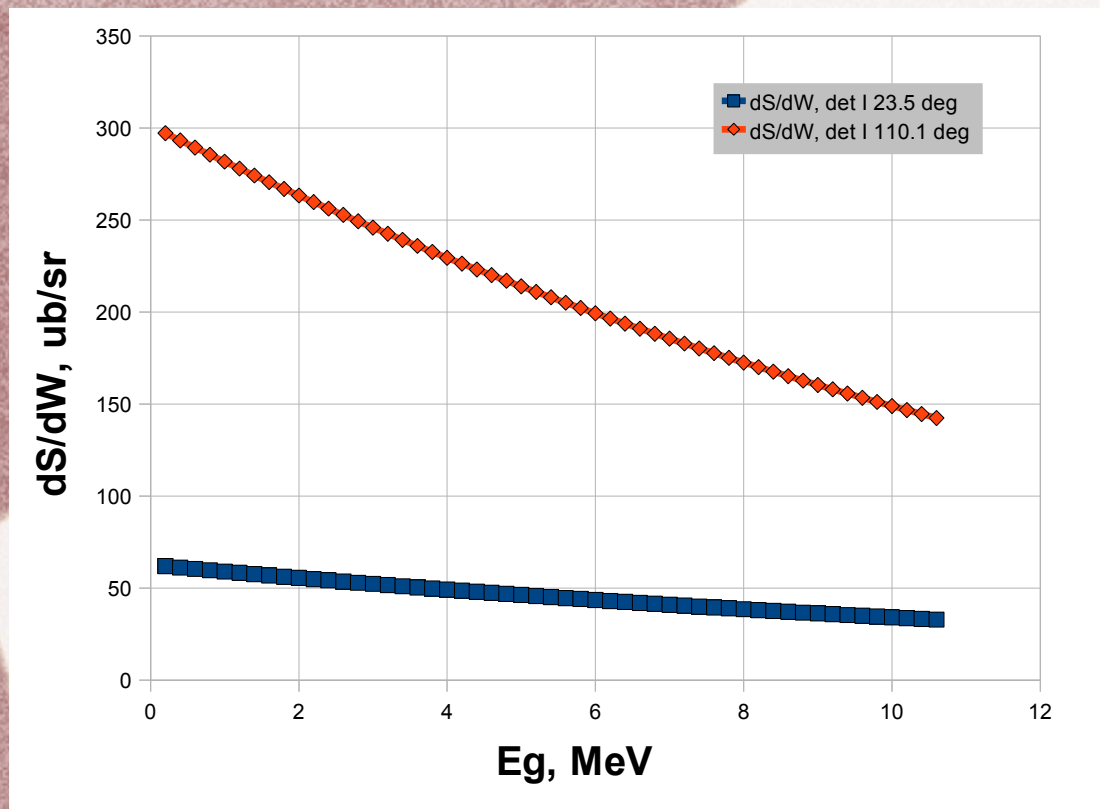


Fig. 9. Differential cross-section of photodisintegration obtained with fitted coefficients from Patrovi's paper.

[***] V. P. Likhachev, M. N. Martins, Yu. A. Kasatkin, M. T. F. da Cruz, J. D. T. Arruda-Neto, R. Guarino, V. B. Shostak, *Disintegration of the Deuteron by Tagged, Linearly-Polarized Photons: Sensitivity of the Differential Cross Sections*, Braz. J. Phys. vol. 27 no. 3 São Paulo Sept. 1997

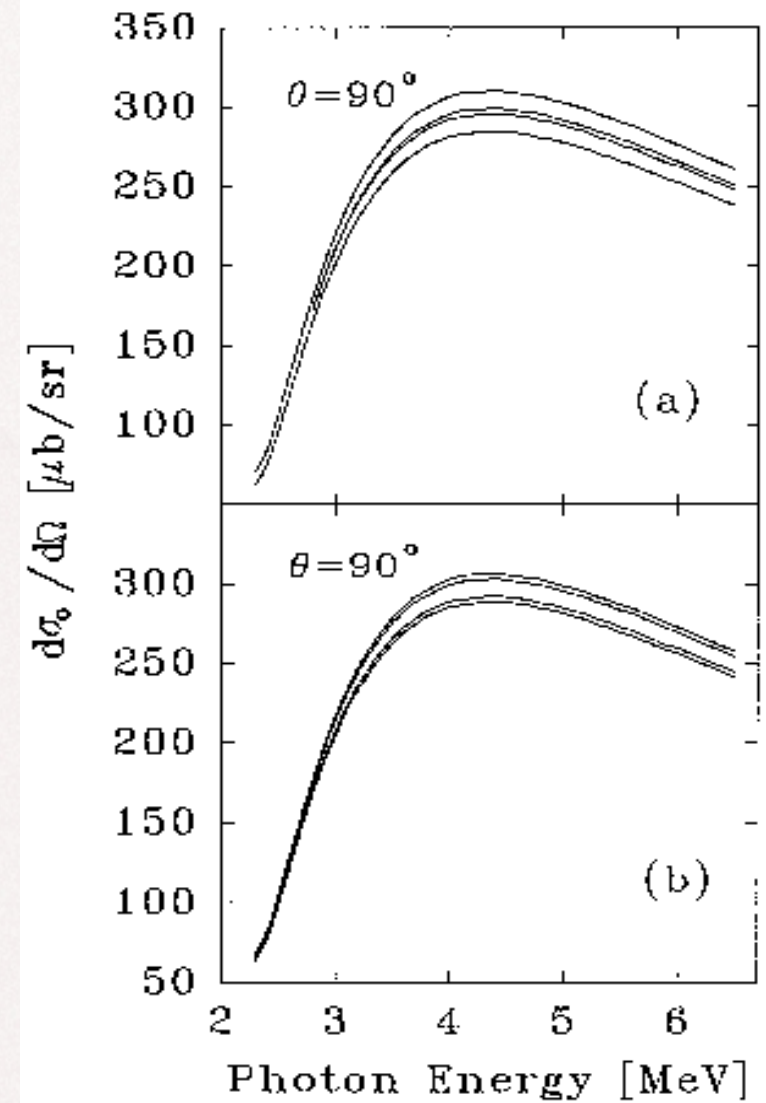


Fig. 10. Differential cross-section of photodisintegration around the reaction threshold [***].

[***]

- "This work shows that, in the near-threshold energy region, where discrepancies between different models do exist, there are no experimental data with enough accuracy to resolve those discrepancies."
- "Angular distributions of differential cross sections, which contain information about the multipolarity of the transitions, are also completely absent."

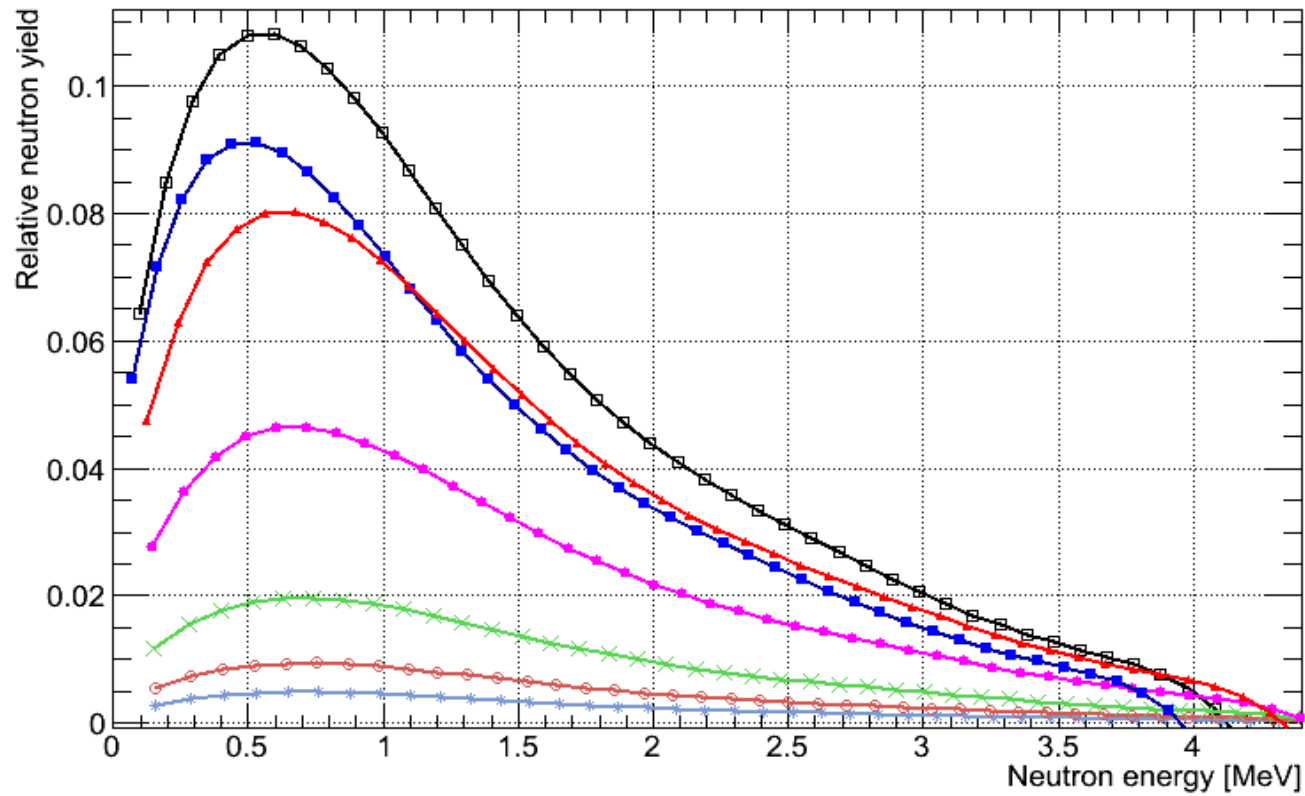


Fig. 11. Relative neutron yield for each of the neutron detectors obtained by weighting the neutron spectra with flux weighted total disintegration crosssection and solid angles.

$$N_{detected}^{Det i} = N_{incident}^{Det i} \cdot \epsilon_i$$

$$N_{detected}^{Det j} = N_{incident}^{Det j} \cdot \epsilon_j$$

$$\frac{N_{incident}^{Det i}}{N_{incident}^{Det j}} = \frac{Area_i}{Area_j}$$

$$\frac{N_{detected}^{Det i}}{N_{detected}^{Det j}} = \frac{Area_i}{Area_j} \cdot \frac{\epsilon_i}{\epsilon_j}$$

$$\frac{\epsilon_i}{\epsilon_j} = \frac{N_{detected}^{Det i}}{N_{detected}^{Det j}} \cdot \frac{Area_j}{Area_i} = k_{ij}$$

$$\epsilon_i = k_{ij} \cdot \epsilon_j$$

The absolute efficiency of Det E was measured to be $\epsilon_E = 14\%$, hence the rest of the efficiencies can be found.

- Partovi's calculation works well in the photon energy region above threshold value of photon energy in the photodisintegration reaction of D2.
- Different model describing differential cross section of D2 photodisintegration reaction near threshold value is needed.
- The efficiency can be defined once the differential cross section is known.